



HAL
open science

Identifying fish spawning grounds by combining catch declarations and scientific survey data

Baptiste Alglave, Youen Vermard, Etienne Rivot, Marie-Pierre Etienne,
Mathieu Woillez

► **To cite this version:**

Baptiste Alglave, Youen Vermard, Etienne Rivot, Marie-Pierre Etienne, Mathieu Woillez. Identifying fish spawning grounds by combining catch declarations and scientific survey data. 2022. hal-03674691v1

HAL Id: hal-03674691

<https://hal.science/hal-03674691v1>

Preprint submitted on 30 May 2022 (v1), last revised 9 Jan 2023 (v2)

HAL is a multi-disciplinary open access archive for the deposit and dissemination of scientific research documents, whether they are published or not. The documents may come from teaching and research institutions in France or abroad, or from public or private research centers.

L'archive ouverte pluridisciplinaire **HAL**, est destinée au dépôt et à la diffusion de documents scientifiques de niveau recherche, publiés ou non, émanant des établissements d'enseignement et de recherche français ou étrangers, des laboratoires publics ou privés.

Identifying fish spawning grounds by combining catch declarations and scientific survey data

Baptiste Alglave^{1,2*}, Youen Vermard¹, Etienne Rivot², Marie-Pierre Etienne³, & Mathieu Woillez⁴

¹ DECOD (Ecosystem Dynamics and Sustainability), IFREMER, Institut Agro, INRAE, Nantes, France

² DECOD (Ecosystem Dynamics and Sustainability), Institut Agro, IFREMER, INRAE, Rennes, France

³ Mathematical Research Institute of Rennes IRMAR, Rennes University, Rennes, France

⁴ DECOD (Ecosystem Dynamics and Sustainability), IFREMER, Institut Agro, INRAE, Brest, France

*corresponding author: email: baptiste.alglave@agrocampus-ouest.fr; present address: DECOD (Ecosystem Dynamics and Sustainability), Institut Agro, IFREMER, INRAE, Rennes, France

Abstract

Identifying and protecting essential fish habitats like spawning grounds requires an accurate knowledge of fish spatio-temporal distribution. Data available through commercial declarations provide valuable information covering the whole year and consequently they could prove useful to identify spawning grounds. We developed an integrated framework to infer fish spatial distribution on a monthly time step by combining scientific and commercial data while explicitly considering the preferential sampling of fishermen towards areas of higher biomass. Over the spawning period, we applied a method to identify areas of persistent aggregation of biomass and interpret these as spawning areas. The model is applied to infer monthly maps of three species (sole, whiting, squids) in the Bay of Biscay on a 9-years period. Integrating several commercial fleets in inference provide a good coverage of the study area and improves model predictions. The preferential sampling parameters give insights into the temporal dynamics of the targeting behavior of the different fleets. Persistent aggregation areas reveal consistent with the available literature on spawning grounds, highlighting that our approach allows to identify potential areas of reproduction.

Keywords: Species distribution model, Spatio-temporal model, Hierarchical model, VMS and logbook data, Fish reproduction areas, Template Model Builder (TMB)

28 **1 INTRODUCTION**

29 Integrating fisheries into Marine Spatial Planning (MSP) to preserve ecosystem functions
30 and ensure a sustainable exploitation requires an accurate knowledge of fish spatio-
31 temporal distribution and more specifically of fish essential habitats such as reproduction
32 and nursery grounds (Janßen et al. 2018). However, such knowledge is still missing for
33 many species due to a lack of data with sufficient spatial, temporal or demographic
34 resolution (Delage and Le Pape 2016; Regimbart et al. 2018).

35 The available data to map fish distribution and identify essential habitats mainly rely on
36 either scientific survey data (fishery-independent data) or commercial data available
37 through on-board observer programs (fishery-dependent data) (Pennino et al. 2016). Both
38 data sources benefit of direct on-board recording of catches and are usually considered
39 as high quality data. Furthermore, both data sources were proved to be complementary
40 (Rufener et al. 2021). Scientific data benefit from a standardized sampling plan, a constant
41 catchability and occur each year at the same period. Consequently, they provide
42 standardized data on a large spatial extent for the most species and size classes (Hilborn
43 and Walters 2013; Nielsen 2015). On the other hand, observer data potentially provide
44 data over the full year for all caught species, even though they do not follow a standardized
45 protocol as survey data. Both are characterized by a relatively low sampling intensity in
46 space and time. Because of material limitations, surveys occur only once or twice a year
47 and provide a limited number of sample each time (ICES 2005) and observer programs
48 only cover a limited fraction of the entire fleet (e.g. only 1% of all sea trips are covered by
49 the French observer programs - Cornou et al., 2021). The low sampling density of both
50 data sources may lead to imprecise predictions (ICES, 2005; Alglave et al., 2022) and

51 constrains to consider only rough temporal resolution (e.g. semesters, quarters or
52 seasons – see for instance Kai et al., 2017; Pinto et al., 2019; Rufener et al., 2021) to
53 ensure a satisfying spatial coverage of the data at each time step. Nevertheless, the
54 temporality of key biological events, such as the reproduction peak, may be much tighter
55 than the temporal resolution of data (Biggs et al. 2021). Hence, those data alone are likely
56 not to provide accurate inferences on essential fish habitats such as spawning grounds.

57 Commercial catch declarations combined with their fishing locations available from VMS
58 (Vessel Monitoring System) were proven to be an interesting alternative to obtain catch
59 per unit effort (CPUE) data with fine spatial and temporal resolution (Pedersen et al. 2009;
60 Bastardie et al. 2010; Gerritsen and Lordan 2010; Hintzen et al. 2012; Murray et al. 2013;
61 Azevedo and Silva 2020). However, considering commercial fisheries data to infer fish
62 spatial distribution remains highly challenging. Among other challenges, this implies
63 accounting for fishermen sampling behavior. Fishermen typically tend to preferentially
64 sample areas of higher biomass (a process referred to as preferential sampling, PS -
65 Diggle et al. 2010) which can lead to biased spatial predictions if not accounted for in
66 inference (Conn et al. 2017; Pennino et al. 2019; Alglave et al. 2022).

67 In a recent paper, Alglave et al. (2022) developed an integrated modelling framework to
68 infer spatial distribution of fish abundance by combining scientific survey and commercial
69 CPUE data from different fishing fleets while accounting for PS in the distribution of fishing
70 effort. They applied their framework to commercial data of a single month to match with
71 the scientific survey, and did not consider any temporal dimension in their model.

72 In this paper, we extend the modeling framework from Alglave et al. (2022) with a temporal
73 dimension to estimate fish spatio-temporal distribution at a monthly time step. Our new
74 model accounts for the variation over time (monthly time step) in the biomass field as well

75 as in the intensity of PS of the distinct fishing fleets. To illustrate the value of the method,
76 we selected and applied the model to 3 demersal species in the Bay of Biscay (common
77 sole, whiting and squids) characterized by contrasted configurations regarding the
78 available knowledge of their spawning grounds. We used those applications to reinforce
79 results obtained in Alglave et al. (2022) demonstrating how the integrated framework
80 benefit from the huge amount of spatio-temporal CPUE data to produce accurate maps of
81 spatio-temporal biomass. To illustrate the capacity of the framework to identify potential
82 spawning grounds, we processed model outputs to identify areas of recurrent aggregation
83 occurring during the reproduction season and confronted these to literature information.

84

85 **2 MATERIAL AND METHODS**

86 In this section, we first present the different species, the datasets and how we process
87 and combine them to produce CPUE data in space and time. Second, we extend the
88 model proposed by Alglave et al. (2022) to introduce a temporal dimension on a discrete
89 monthly time step. Then, we illustrate how integrating several fleets in the analysis
90 improves models predictions, how the PS component modifies model predictions and can
91 be interpreted. Last, we illustrate how we investigate spatio-temporal dynamics from
92 model outputs and identify reproduction grounds based on the aggregation patterns of
93 each 3 species. The models were fitted to data from 2010 to 2018 on a monthly time step
94 (108 time steps).

95 **2.1 Case studies**

96 Sole is a data-rich case. Direct information about reproduction grounds is available
97 through egg and larvae surveys (Arbault et al. 1986). Discard rates is also very low, which
98 makes the landings data a good proxy of the catch (ICES 2019a). Whiting is a data-poor
99 case study where only indirect information of reproduction period exists through spring
100 trawl surveys (House and Forest 1993). Discard rates can be high (about 30 %) and thus
101 landings data may provide a biased picture of the real catches (ICES 2019b). Squids
102 represent a mixture of several species: *Loligo Vulgaris* (Lamarck, 1798), *Loligo forbesii*
103 (Steenstrup, 1856) and *Alloteuthis sp* (Lamarck, 1798). They are declared under a
104 common denomination in the catch (Loliginidae here referred as squids). Overall scientific
105 survey suggest that the predominant species in the Bay of Biscay is *Loligo Vulgaris* (ICES,
106 2020a, p.17). All 3 species are data-poor: no information exist regarding their reproduction
107 grounds but some information of the reproduction period exist for *Loligo Vulgaris* (Moreno
108 et al. 2002).

109 **2.2 Data**

110 **2.2.1 High spatial resolution catch per unit effort data for the mature component**
111 **of the populations**

112 We pre-processed the VMS and catch declaration (logbook) data to obtain high spatial
113 resolution CPUE data for the mature component of those three stocks, for three different
114 fishing fleet, and for each month of the 2010-2018 time series. In the text, CPUE is used
115 but no discard information is available at the scale of the fishing sequence.

116 We selected data of three trawlers métiers OTB_DEF (bottom otter trawl targeting
117 demersal species), OTB_CEP (bottom otter trawl targeting cephalopods) and OTT_DEF
118 (multi-rig otter trawl targeting demersal species). Here the term fleets is used to refer to
119 these groups. They refer to distinct component that have overall similar targeting
120 behaviors and similar technical characteristics. These fleets were selected (1) so as to
121 cover the full spatial domain (Figure 1) and (2) because fishing time of trawlers is a good
122 proxy of effort which allows to compute reliable CPUE for biomass (Hovgêrd and Lassen
123 2008).

124 Because one of our primarily goal is to identify spawning grounds, we filtered only the
125 mature fraction of the landings. This was done by crossing the landings data with length
126 class and maturity data (see details in SM1). Note that this procedure was not possible
127 for squids, as there are no data on maturity and size classes in this case.

128 Landing data were then combined with VMS data to finally obtained high spatial resolution
129 CPUE data discretized on a $0.05^{\circ} \times 0.05^{\circ}$ grid on a monthly time step (see the detailed
130 procedure for this combination in Alglave et al. (2022) and SM2).

131 **2.2.2 Scientific data**

132 We also integrated scientific data in the analysis. For hake and squids we used the survey
133 data from the EVHOE survey. The Orhago survey was used for sole (ICES, 2020 - see
134 SM, Figure S3). The data were extracted from the DATRAS database on the period 2010
135 - 2018. Only the mature fraction of the survey catches were kept in the analysis to make
136 it comparable with commercial data. Some details on the surveys are given in SM3.

137 **2.3 Spatio-temporal integrated model**

138 We build on the integrated hierarchical model proposed by Alglave et al. (2022) by
139 incorporating a temporal component to model the evolution of the latent field of biomass
140 across the monthly time steps (Figure 2). The PS of commercial data for the different
141 fleets is modelled explicitly through inhomogeneous Poisson point processes for the
142 fishing locations.

143 **2.3.1 Biomass field**

144 As a notable extension of Alglave et al. (2022), the biomass field (eq.1) is modelled as a
145 spatio-temporal Gaussian Random Field (GRF) through a log link as:

$$146 \quad \log(S(x, t)) = \alpha_s(t) + \delta(x, t) \quad (1)$$

147 where $x \in D \subset R^2$ stands for the spatial locations and $t \in \llbracket 1, T \rrbracket$ the monthly time steps.
148 The term $\alpha_s(t)$ is a time varying intercept modelled as a fixed effect and $\delta(x, t)$ is a GRF
149 spatio-temporal process which represents the spatio-temporal correlation structure of the
150 biomass field. As commercial data may not always cover the full area, the temporal
151 correlation component allows to interpolate between time-steps. Here, the spatio-temporal
152 term has a classical stationary first-order autoregressive form (eq.2) following (Cameletti
153 et al. 2013):

$$154 \quad \delta(x, t) = \varphi \cdot \delta(x, t - 1) + \omega(x, t) \quad \text{for } t = 2, \dots, T \quad (2)$$

155 The autocorrelation coefficient φ is a scalar with $\varphi \in] - 1,1[$, $\omega(x, t)$ represents the spatial
156 innovation and is a 0 mean GRF (with no temporal correlation).

157 Note that no covariate is included in the latent field to keep the model as simple as
158 possible. If any, the covariates effects are captured through the spatio-temporal term
159 $\delta(x, t)$. Similarly, the intercept $\alpha_S(t)$ was modelled through a simple fixed effect but more
160 complex specifications including some seasonal, yearly and interaction effect could be
161 adopted such as in Thorson et al. (2020).

162 **2.3.2 Sampling process for the commercial fishing points**

163 As the scientific survey sampling plan is designed independently from the biomass field,
164 scientific sampling locations do not need to be modelled explicitly (Diggle et al. 2010). By
165 contrasts, the dependence between the fishing locations and the biomass field has to be
166 modelled to capture preferential sampling. We extended the model proposed by Alglave
167 et al. (2022) to account for temporal variations in PS. Fishing locations are modelled as
168 an inhomogeneous point process (X_{comj} in the Figure 2) whose intensity $\lambda_j(x, t)$ (eq.3)
169 controls the expected number of fishing points within a given area:

$$170 \quad \log(\lambda_j(x, t)) = \alpha_{X_j}(t) + b_j(t) \cdot \log(S(x, t)) + \eta_j(x, t) \quad (3)$$

171 where:

- 172 - the time varying intercept $\alpha_{X_j}(t)$ quantifies the average fishing intensity on the
173 whole area; as the biomass intercept $\alpha_S(t)$, it is modelled as a fixed effect;
- 174 - the time varying $b_j(t)$ quantifies the strength of PS; it is modelled as a fixed effect
175 too. If $b_j(t) = 0$, then PS is null. If $b_j(t) > 0$, then PS occurs and the greater, the
176 stronger PS;

177 - the pure spatial GRF $\eta_j(x, t)$ captures the remaining spatial variability in the fishing
178 point pattern not captured by the PS term (for instance, dependence of the fishing
179 locations towards management regulations, distribution of other targeted species,
180 habits/tradition).

181 **2.3.3 Observation process**

182 All observations for both scientific and commercial data of any fleet j are assumed all
183 mutually independent conditionally on the latent field of biomass and the sampling
184 locations. The observation model allows to distinguish several fleets with specific
185 catchabilities. As data (both scientific and commercial) eventually present a high
186 proportion of zero values, we model the observations through a Poisson-link zero-inflated
187 model introduced by Thorson (2018) and already used in Alglave et al. (2022) (see
188 detailed description of the observation model in SM4).

189 **2.3.4 Maximum likelihood estimation**

190 The estimation of the spatio-temporal model is achieved through maximum likelihood
191 estimation. We used the SPDE approach Lindgren et al. (2011) and Template Model
192 Builder (TMB - Kristensen et al., 2016) for a fast estimation of the spatial and spatio-
193 temporal random effects. Details on estimation are provided in SM 5, 6 and 7.

194 **2.4 Evaluating the Interest of integrating multiple fleets**

195 Integrating several fleets in inference allows to cover the whole area (Figure 1) and is
196 expected to improve inferences. To illustrate the value of integrating the data from multiple
197 fleets within a single integrated model, we compared the spatial predictions obtained by
198 fitting the model to all available data with those obtained by integrating only one fleet. In
199 addition, we investigated if integrating all the fleets in inference increased the correlation

200 between scientific data and model predictions. We also compared the coefficient of
201 variation of the prediction between each model (for November 2018).

202 **2.5 Evaluating the value of modelling PS**

203 We first assessed the impact of PS on the distribution of biomass by comparing
204 estimations obtained from integrated models (i.e. models fitted to all data sources)
205 accounting for PS with those obtained when ignoring PS. We computed the log-likelihood
206 related to each data source (commercial and scientific data) to assess if there is an
207 improvement in model goodness-of-fit when accounting or not for PS. Note that fitting a
208 model without PS is straightforward as it only requires to remove the sampling process
209 component from the likelihood function.

210 **2.6 Interpreting the intensity of preferential sampling**

211 The estimates of PS parameters may bring valuable information on the dynamics of the
212 fishery as they inform on the strength of the relationship between commercial sampling
213 distribution and species distribution. We investigate the variability of the PS parameters
214 (*b*) by representing the variability of the different *b* parameter estimates for the three case
215 studies and the different fleets. Then, focusing on the sole case study, we highlight the
216 insights brought by the model on the temporal evolution of PS and its seasonal variations.

217 **2.7 Investigating spatio-temporal dynamics and identifying reproduction** 218 **grounds**

219 The spatio-temporal model provides some insight on the temporal dynamics of species
220 distribution both at inter- and intra-annual levels. Based on the maps of abundance
221 inferred at each time steps, we applied a method to identify recurrent aggregation areas.

222 **2.7.1 Aggregation index**

223 We used the Getis and Ord index $G_d(x, t)$ (Getis and Ord 1992; Ord and Getis 1995) to
224 determine persistent aggregation areas (see for instance Milisenda et al., (2021)). The
225 generalized version of the Getis and Ord index is given in Bivand and Wong (2018) and
226 Ord and Getis (1995). Basically, $G_d(x, t)$ is a normalized version of the ratio between the
227 sum of the log-biomass (denoted $s(x, t)$) within a fixed neighborhood d and the sum of
228 $s(x, t)$ on the entire area (for a fixed time step) (Getis and Ord 1992). We computed these
229 indices on $s(x, t) = \log(S(x, t))$ so that the $s(x, t)$ are Gaussian, which makes G_d
230 Gaussian too. In the application, we used a neighborhood distance $d=7.5$ km which
231 defines a small neighborhood of 8 cells (the direct neighbors of each cell grid) and allows
232 to identify very localized aggregation areas. Positive values for the aggregation index G_d
233 indicates that $s(x, t)$ fall within a local patch of high values while negative G_d indicates
234 that $s(x, t)$ fall within a local patch of low values. Near 0 values G_d , indicates that $s(x, t)$
235 does not fall in some local aggregation patch. As G_d follows a standardized Gaussian
236 distribution, the comparison between the value of the index and the quantiles of a standard
237 Gaussian distribution can be used to evaluate whether or not the latent field of biomass
238 fall within a statistically significant high or low aggregation patch. We used the quantile
239 99% (2.58) as a threshold to ensure a high level of significance for patch detection (only
240 local patch of positive values are considered) and applied the Bonferroni correction to
241 account for the multiple statistical tests that are conducted.

242 Then, we define the persistence indices $IP(x, m)$ as the proportion for which a point x falls
243 significantly within an aggregation area for a specific month/season m (can be either a
244 month or several months) among several years. IP allows to define the persistent

245 aggregation areas during reproduction throughout the time series. They are used in the
246 following to identify reproduction grounds.

247 **2.7.2 Confronting the results with the available literature**

248 We compare the information available from the literature (for sole and whiting) with the
249 persistence indices on their reproduction periods.

250 Arbault et al. (1986) investigated the reproduction of sole along the Bay of Biscay based
251 on several egg surveys occurring in 1982. Five surveys were conducted between January
252 and May. Egg density was sampled in different locations from Hendaye to Pointe du Raz
253 (43°30N-48°N) and allowed to map the distribution of egg production on the full study
254 domain. The pic of reproduction occurred in February; thus we compare the maps
255 obtained from the February survey with the persistence index we obtained for February.

256 For whiting, only two EVHOE trawl surveys occurred during spring (considered as the
257 reproduction period of whiting) between 1987 and 1992 in the Bay of Biscay (House and
258 Forest 1993). For each haul, the individuals were counted and aged. Individual up to two
259 years were all considered mature. We compare the distribution of age-2 individuals
260 obtained with these surveys (there were very few age 3-individuals) and the index of
261 persistence from our model during spring (March to May).

262 No available information exists regarding the reproduction grounds of squids in this area,
263 however the study from Moreno et al. (2002) investigated the reproduction period for
264 *Loligo vulgaris* in the Eastern Atlantic and highlighted that their reproduction falls in winter
265 and spring with a pic from January to April. We compute the persistence index for this
266 period to evidence if some spatial aggregation patterns emerge from the model outputs
267 and could be considered as spawning grounds.

268 To assess whether the aggregation patterns within the reproduction period are stable over
269 the time period, we iteratively computed the persistence index over a 5-year mobile time-
270 span while pushing forward one year each time.

271 **3 RESULTS**

272 **3.1 Assessing the contribution of each data sources to inference**

273 Results highlight how combining several commercial fleets in the framework brings a
274 better picture of the spatial distribution on the whole domain. For instance, when
275 comparing model prediction the month of the survey and survey outputs, integrating
276 several fleets into the analysis improves correlation with scientific data (Figure 3). It also
277 allows to reduce the standard deviation of the predictions on the full domain (Figure S8).
278 When looking at the predictions within the spatial range of the fleets, single-fleet models
279 logically provide similar spatial predictions compared with the integrated model (Figure 4;
280 red dots). However, predictions realized outside the spatial range of the fleet largely depart
281 from the ones realized through the integrated models (black dots, Figure 4), emphasizing
282 that the other fleets bring additional information to inference in these areas. This is
283 particularly evidenced with the OTB_CEP and OTT_DEF fleets that partially cover the
284 study area compared with OTB_DEF that better cover the whole study area (Figure 1).

285 **3.2 Interpreting estimates PS intensity**

286 Estimates of the PS intensity (b parameters) for the different species, the different fleets
287 and the different time steps provide information on the targeting behavior which are
288 consistent with expertise. Estimates of b are positive for each species and each fleet
289 (Figure 5, left column). For squids, PS is the strongest for OTB_CEP followed by
290 OTB_DEF and OTT_DEF. This is consistent with the expert knowledge of the targeting
291 behavior of these fleets: OTB_CEP target cephalopods and catch on average 15% of
292 squids while OTB_DEF and OTT_DEF catch respectively 5% and 1% of squid). A similar
293 pattern can be identified for whiting ($b_{OTB_CEP} > b_{OTB_DEF} > b_{OTT_DEF}$); this is consistent
294 with species spatial distribution as whiting (like squids) are found in coastal areas where

295 the OTB_CEP fleet is operating. For sole, the strength of PS is on average higher for
296 OTB_CEP and OTT_DEF than for OTB_DEF but with less contrast between the three
297 commercial fleets.

298 Interestingly, some of the b parameters time series emphasize seasonal patterns (Figure
299 6, top). For instance in the sole case study for the OTB_CEP fleet, the b parameters are
300 higher in summer and autumn emphasizing relatively stronger PS, while being lower in
301 winter and early spring (but see section 3.4 below for a more detailed interpretation of this
302 seasonality pattern).

303 **3.3 Evaluating the influence of PS on spatial distribution**

304 Because estimates of b are positive, spatial density of fishing points is positively correlated
305 with biomass density. Hence, considering PS revises downwards the biomass estimates
306 in areas not sampled by the commercial fleets compared to estimates obtained while
307 ignoring PS (Figure 5, right column, black points), but does not strongly affect predictions
308 in locations within the range of the fleets (blue points). Considering PS only slightly
309 improves the fit of the model to the data. For the Sole case study, some improvement of
310 the likelihood occurred in both the commercial and the scientific likelihood values (Table
311 1). For whiting and squids, there are no strong modifications in both scientific and
312 commercial likelihoods.

313 **3.4 Investigating spatio-temporal dynamics of fish biomass**

314 Results provide biomass density maps on a monthly time step that allow for evaluating
315 seasonal distribution patterns, and from which aggregation index were calculated. The
316 temporal correlation parameter (φ) is estimated around 0.8 for all the species emphasizing
317 strong temporal correlations in the biomass field values. The range parameters are

318 estimated to 55 km for sole and squids while being estimated to 67 km for whiting
319 emphasizing wider spatial autocorrelation for this species.

320 Concerning the Sole case study, model predictions highlight the relatively offshore
321 distribution from November to April and its coastal distribution from June to October
322 suggesting some migrations happen between these 2 periods (Figure 6, bottom). In
323 particular, the migration in June/July conducts to a contraction of the sole distribution
324 around the Vendée coast, the Gironde Estuary and the Landes coast (45.5°N-46°N) while
325 the migration in November leads to an expansion of the species distribution towards the
326 offshore areas all along the Bay of Biscay. Interestingly such seasonality coincides with
327 the seasonality of PS intensity for the OTB_CEP (Figure 6, Top). Higher PS parameters
328 corresponds to coastal distribution of sole while lower PS parameters corresponds to
329 offshore distribution of sole.

330 Similar maps can be computed for the other species and are presented in SM10.

331 **3.5 Aggregation index and reproduction grounds**

332 Regarding spawning grounds, both sole and squids emphasize strong aggregation
333 patterns that match the available knowledge of their reproduction grounds. For sole, the
334 aggregation areas globally match with the observed area of maximum egg concentration
335 (Figure 7), although reproduction grounds are slightly eastern in the case of egg maps.
336 This slight discrepancy could be interpreted as an effect of the larval drift as the maps
337 provided by Arbault et al. (1986) are concentration of eggs and not reproduction grounds
338 per se. Overall, these aggregation areas are stable over time (Figure 8).

339 For whiting, similar patterns can be identified during the reproduction period (Figure 7);
340 they match with previous studies investigating the spatial distribution of mature whittings

341 (House and Forest 1993). In particular, the Northern (3°W - 47°N) and the Southern (2°W -
342 45.5°N) aggregation patches are almost systematically significantly considered as
343 aggregation areas (aggregation index equals 1) while the other middle one (2.5°W -
344 46.5°N) is classified as an aggregation area that appears less frequently. An additional
345 persistent aggregation area can be identified in the North of the Bay of Biscay (4.5°W -
346 48°N) suggesting that reproduction may also occur in this area which was not identified in
347 the report of House and Forest (1993). Interestingly the Northern aggregation area (3°W -
348 47°N) is more pronounced at the end of the period (Figure 8).

349 For squids, no literature information related to any reproduction ground exist, only the time
350 period of the reproduction is known (the pic fall between January to April). On this time
351 period, some persistent aggregation areas can be evidenced in coastal areas (Figure 7)
352 along the Vendée coast (2.5°W - 46.5°N), the Landes coasts (1.5°W - 44°N to 45°N) and
353 around Belle-Île-en-Mer (3°W - 47.25°N). Interestingly the two Northern aggregation areas
354 are more pronounced at the end of the time series compared to the beginning of the time
355 series (Figure 8).

356 Similar maps of persistent aggregation areas are available for each month and evidence
357 some other aggregation areas outside of the reproduction period (SM11). For instance,
358 for sole a persistent patch can be identified offshore the Gironde Estuary (1.5°W – 45.5°N)
359 from August to December.

360

361 **4 DISCUSSION**

362 **Main findings**

363 In this paper, we develop a framework to infer fish spatio-temporal distribution on a
364 monthly time step while combining scientific survey data and commercial catch
365 declarations from several fleets. Commercial catch data constitute a valuable data source
366 that complement scientific survey or onboard sampling programs by providing much
367 higher spatio-temporal sampling density. Those complementary sources of data were
368 integrated through a spatio-temporal hierarchical model taking into account spatio-
369 temporal variation within the biomass field and PS on a monthly time step. We fitted the
370 model to VMS-logbooks data filtered and processed over the period 2010-2018 for 3
371 demersal species (sole, squids and whiting) in the Bay of Biscay.

372 We emphasize the benefit of integrating several spatially complementary fleets to infer
373 fish distribution throughout the year. We demonstrate how the within year dynamic of the
374 PS parameters can be interpreted in regards to the joint dynamics of species distribution
375 and effort distribution and to the overall targeting behavior of the fleets (e.g. OTB_CEP for
376 the squids case study). Even though PS parameters are not fishing intention per se
377 (Bourdaud et al. 2019), these could advantageously complement information provided by
378 landing profiles to estimate the targeting behavior of any group of vessels (either
379 métier/fleet or any group that would seem appropriate).

380 Interestingly, although interpretation of the PS parameters provide insight into the spatio-
381 temporal fleet dynamics, accounting for PS in the inferences does not significantly improve
382 model fitting even when some fleets emphasize strong PS (e.g. squids, OTB_CEP). These
383 results contrasts with Alglave et al. (2022), and could result from the integration of several

384 fleets in the analysis that allow a full coverage of the area. Indeed, in Alglave et al. (2022),
385 the fleet emphasizing strong PS only covered a restricted (and coastal) part of the area.
386 As introducing PS mainly affects inferences on poorly sampled areas, predictions in the
387 offshore areas were mostly affected. Here, as the fleets are all estimated to have a
388 positive PS and cover the whole area, PS only downscale the predictions in the few areas
389 areas that remain unsampled.

390 Filtering the mature fraction of the population in both the scientific and the commercial
391 data allow us to infer the spatio-temporal distribution of the mature fraction of the biomass
392 through the year on a monthly time step. We developed an index to infer aggregation
393 areas of the mature fraction of the biomass that are persistent across years. When
394 calculated on a temporal window predefined following the available information on the
395 reproduction period for each species, the aggregation index allow us to identify the main
396 recurrent spatial aggregation areas within the reproduction period. Results demonstrate
397 that the recurrent aggregation areas identified from our method for Sole and Whiting were
398 highly consistent with those already identified in the literature. Our results demonstrate
399 how the aggregation index can provide new insights on the spawning grounds for species
400 like squids for which no information on the spawning grounds is available on the literature.
401 Areas of high aggregation persistent across years were identified during the expected
402 period of reproduction and could be interpreted as spawning grounds. This opens
403 perspectives for applying more systematically the approach for species where no
404 information of reproduction grounds is available to fill the gaps in our knowledge with
405 minimum cost (Delage and Le Pape 2016; Regimbart et al. 2018).

406

407

408 **Combining our results with other data sources to refine inferences on spawning**
409 **grounds**

410 Although the mature fraction of the biomass was filtered in the data, our maps do not
411 directly inform whether individuals are actually reproducing or not. Persistent aggregation
412 areas should be considered as potential spawning areas rather than actual spawning
413 areas. To get information on actual reproduction zones and support our findings, other
414 kind of data could complement our analysis. Typically, our maps could be of great help to
415 design surveys recording eggs, larvae and spawning individuals that would provide direct
416 information of species reproduction (Fox et al. 2008). Because developing such additional
417 surveys would be highly expensive, our maps could provide valuable a priori information
418 to optimize the survey design and potentially find a compromise between the cost, the
419 spatial extent, the temporal coverage of the survey and the accuracy of the expected
420 estimates/predictions. Similar ideas were already applied to the sole case study to
421 investigate more precisely the space-time variation of sole reproduction. Arbault et al.
422 (1986) work provided a priori information of reproduction grounds that allowed designing
423 more localized surveys to study inter- and intra-annual variability of one specific sole
424 spawning area (Petitgas 1997). Several statistical methods have been developed since
425 and are suitable to optimize such adaptive sampling design; see for instance the recent
426 work of Leach et al. (2021).

427 Our results could also be combined with fishermen expert knowledge (Yochum et al. 2011)
428 to complement our knowledge of fish reproduction (Delage and Le Pape 2016). For
429 instance, Bezerra et al. (2021) and Silvano et al. (2006) proved the usefulness of fishers
430 knowledge to determine the temporality of fish spawning and to identify some spawning
431 grounds by crossing the information of aggregation areas provided by several fishermen.

432 These were proved complementary with scientific data as they can be available at low
433 cost and provide local knowledge of fish ecology.

434 **Limits and perspectives for the approach**

435 Our framework has several limitations that are all material for future research avenues.

436 First, our model remains relatively simple in regards to all the temporal processes that
437 actually occur within a fishery. It is both a strength and a weakness: such way the model
438 remains relatively generic, but one might want to extend it further to account for other
439 temporal and spatio-temporal processes affecting fisheries dynamics. For instance, we
440 opted for a non-seasonal representation of the model, however one could make it
441 seasonal by decomposing the intercepts $\alpha_s(t)$ and $\alpha_{x_j}(t)$ as well as the random effects
442 $\delta(x, t)$ and $\eta(x, t)$ into seasonal and yearly terms in addition to some 'season x year'
443 interaction terms as is performed in Thorson et al. (2020). In their work, such specification
444 mainly allowed to provide information over the time-steps where data was lacking. In the
445 configuration of our case studies, data is available for all time steps and have a relatively
446 good coverage of the study domain. Consequently, such model specification should not
447 modify the overall inference of the biomass field we obtain even though it provide a nice
448 conceptual view of seasonality. Alternatively, our framework could integrate orthogonal
449 spatio-temporal terms in the latent field to capture the main mode of variability of the
450 biomass field (Thorson et al. 2020b). Such orthogonal terms would allow to capture the
451 main spatial patterns that structure the latent field as well as their variation in time. These
452 could prove very useful to identify the structuring processes that affect species distribution
453 and could give a valuable insight in the space-time dynamics of the species. Another
454 exciting research avenue would consist in integrating population dynamics in the latent

455 field of biomass (Cao et al. 2020). This would require to refine further the demographic
456 resolution of the VMS-logbooks data (see for instance Azevedo and Silva 2020), but once
457 done, it would give access to huge data for inferring the space-time dynamics of fish
458 populations. Finally, our model considers fishermen preferentially sample areas where the
459 biomass is higher (preferential sampling), but does not consider any other drivers and
460 specifically the temporal and spatio-temporal relations that can affect fishers behavior.
461 These can be highly complex and may depend on the distribution of the resource,
462 tradition/habits, management regulations (Abbott et al., 2015; Girardin et al., 2017; Salas
463 and Gaertner, 2004; Hintzen, 2021). These drivers are rarely studied in both space and
464 time (although see Tidd et al., 2015). Our framework could allow to jointly model the
465 dynamics of the species, the distribution of the effort, the link that relates species
466 distribution and effort in space/time and all the other spatial and/or temporal drivers that
467 affect the distribution of fishing effort. For instance, we could relate the fishing intensity to
468 the biomass field from the previous time steps, or alternatively consider that the locational
469 choice depend on the catches of the previous time steps. Adding such covariates and
470 spatio-temporal dependencies in the sampling equation (eq.3) will probably not modify the
471 overall pattern of biomass distribution, but it would allow to quantify the drivers of
472 fishermen behavior and give valuable insight in the functioning of the fishery.

473 Second, including discards would potentially improve our approach. Indeed, logbooks
474 data are landings declarations data which means they inform on the landings and not on
475 the true catch. Thus, by assuming the observations we derive from logbooks data are
476 representative of the biomass, we make the hypothesis that the discard rate is constant
477 in space and time and does not affect model predictions. This should not be a problem for
478 sole and squids as the discards are low and TAC have not been really binding during the

479 studied period. However, the issue might be more stringent for whiting and/or other
480 species with a high and non stationary level of discards. Integrating discards data in the
481 analysis could help solving this issue. Stock et al. (2019) and Yan et al. (2022) used
482 observer data to model bycatch in both space and time and Breivik et al. (2017) used
483 bycatch data from onboard surveys to predict the temporal evolution of bycatch realized
484 in the full commercial data. Similarly, we could integrate into the same analysis the
485 logbooks and the observer data by assuming that the catch of observer data is a
486 summation of both landings (which is also observed in the logbooks data) and discards
487 (which is unobserved in the logbooks data). This way, the discards information available
488 from observer data would be shared with the logbooks data and would allow correcting
489 for the missing portion of catch declarations data while possibly accounting for possible
490 space or time variation in the discard rate.

491 Last, our analysis rely on the hypothesis that the spawning season is known a priori.
492 Extending the approach to infer the spawning season based on the temporal dynamic of
493 the aggregation patterns could improve our knowledge of species spatio-temporal
494 distribution. In particular, identifying the main species phenomenological phases and their
495 consistency (or shift) in time is crucial in the context of global change (Thorson et al.
496 2020a).

497 In our study, we computed the aggregation index on a period we assumed to be the
498 reproduction period based on literature (Arbault et al. 1986; Houise and Forest 1993;
499 Moreno et al. 2002). Hence, our results are sensitive to this a priori hypothesis, or our
500 approach can even be inapplicable for species when no information is available in the
501 literature. Several methods exist and could be adapted to extract the spatial patterns that
502 shape model outputs, their related temporal variation and identify from these the main

503 phenological phases that characterize species distribution (e.g. reproduction, feeding -
504 see for instance Empirical Orthogonal Functions or Principal Oscillation Patterns - Cressie
505 and Wikle 2015; Wikle et al. 2019).

506 **Future use for Marine Spatial Planning**

507 Finally, our approach could reveal useful in the context of Marine Spatial Planning (MSP).
508 Janßen et al. (2018) highlighted that one of the main requirement for implementing MSP
509 while accounting for fish ecology is the availability of fine scale information on species
510 distribution and of their essential habitats. Here we propose a method which can provide
511 such information for the fraction of the population available through catch declarations (i.e.
512 mainly the adult fraction and in some cases part of the juvenile fraction). This knowledge
513 is typically needed to design Marine Protected Areas (MPA – see for instance Lambert et
514 al. (2017) or Loisel et al. (2003)), Fishery Conservation Zones (Delage et Le Pape,
515 2016 ; Regimbart et al., 2018), or alternatively identify areas that should be kept for fishing
516 in a context where many other human activities are competing in space and time with
517 fishing (Campbell et al. 2014; Bastardie et al. 2015). This would require to open the
518 spectrum of the analysis to an economical dimension and possibly integrate our results
519 into ecological–economic models in order to evaluate alternative management regulations
520 and assess their tradeoffs in regards to all the sets of ecosystem services provided
521 through activities such as fishing, aquaculture, energy, shipping, recreation and
522 conservation (Nielsen et al. 2018).

523

524 **ACKNOWLEDGMENT**

525 The authors acknowledge the Pôle de Calcul et de Données Marines (PCDM;
526 [https://wwz.ifremer.fr/en/Research-Technology/Research-Infrastructures/Digital-
527 infrastructures/Computation-Centre](https://wwz.ifremer.fr/en/Research-Technology/Research-Infrastructures/Digital-
527 infrastructures/Computation-Centre)) for providing DATARMOR supercomputer on which
528 the model has been fitted.

529 The authors are grateful to the Direction des pêches maritimes et de l'aquaculture (DPMA)
530 and Ifremer (Système d'Informations Halieutiques - SIH) who provided the aggregated
531 VMS and logbooks data. The findings and conclusions of the present paper are those of
532 the authors.

533 **DATA AVAILABILITY STATEMENT**

534 Survey data are available through the DATRAS portal ([https://www.ices.dk/data/data-
535 portals/Pages/DATRAS.aspx](https://www.ices.dk/data/data-
535 portals/Pages/DATRAS.aspx)) with the package 'icesDatras' ([https://cran.r-
536 project.org/web/packages/icesDatras/index.html](https://cran.r-
536 project.org/web/packages/icesDatras/index.html)). Logbooks and VMS data are
537 confidential data and they are available on specific request to DPMA.

538 **REFERENCES**

- 539 Abbott, J., Haynie, A., and Reimer, M. 2015. Hidden Flexibility: Institutions, Incentives, and
540 the Margins of Selectivity in Fishing. *Land Economics* **91**: 169–195.
541 doi:10.3368/le.91.1.169.
- 542 Alglave, B., Rivot, E., Etienne, M.-P., Woillez, M., Thorson, J.T., and Vermard, Y. 2022.
543 Combining scientific survey and commercial catch data to map fish distribution. *ICES*
544 *Journal of Marine Science: fsac032*. doi:10.1093/icesjms/fsac032.
- 545 Arbault, P.S., Camus, P., and Bec, C. le. 1986. Estimation du stock de sole (*Solea vulgaris*,
546 Quensel 1806) dans le Golfe de Gascogne à partir de la production d'œufs. *Journal of*
547 *Applied Ichthyology* **2**(4): 145–156. doi:10.1111/j.1439-0426.1986.tb00656.x.
- 548 Azevedo, M., and Silva, C. 2020. A framework to investigate fishery dynamics and species
549 size and age spatio-temporal distribution patterns based on daily resolution data: a

550 case study using Northeast Atlantic horse mackerel. *ICES Journal of Marine Science*
551 **77**(7–8): 2933–2944. doi:10.1093/icesjms/fsaa170.

552 Bastardie, F., Nielsen, J.R., Eigaard, O.R., Fock, H.O., Jonsson, P., and Bartolino, V. 2015.
553 Competition for marine space: modelling the Baltic Sea fisheries and effort
554 displacement under spatial restrictions. *ICES Journal of Marine Science* **72**(3): 824–
555 840. doi:10.1093/icesjms/fsu215.

556 Bastardie, F., Nielsen, J.R., Ulrich, C., Egekvist, J., and Degel, H. 2010. Detailed mapping of
557 fishing effort and landings by coupling fishing logbooks with satellite-recorded
558 vessel geo-location. *Fisheries Research* **106**(1): 41–53.

559 Bezerra, I.M., Hostim-Silva, M., Teixeira, J.L.S., Hackradt, C.W., Félix-Hackradt, F.C., and
560 Schiavetti, A. 2021. Spatial and temporal patterns of spawning aggregations of fish
561 from the Epinephelidae and Lutjanidae families: An analysis by the local ecological
562 knowledge of fishermen in the Tropical Southwestern Atlantic. *Fisheries Research*
563 **239**: 105937.

564 Biggs, C.R., Heyman, W.D., Farmer, N.A., Kobara, S., Bolser, D.G., Robinson, J., Lowerre-
565 Barbieri, S.K., and Erisman, B.E. 2021. The importance of spawning behavior in
566 understanding the vulnerability of exploited marine fishes in the US Gulf of Mexico.
567 *PeerJ* **9**: e11814.

568 Bivand, R.S., and Wong, D.W.S. 2018. Comparing implementations of global and local
569 indicators of spatial association. *TEST* **27**(3): 716–748. doi:10.1007/s11749-018-
570 0599-x.

571 Bourdaud, P., Travers-Trolet, M., Vermard, Y., and Marchal, P. 2019. Improving the
572 interpretation of fishing effort and pressures in mixed fisheries using spatial overlap
573 metrics. *Can. J. Fish. Aquat. Sci.* **76**(4): 586–596. doi:10.1139/cjfas-2017-0529.

574 Breivik, O.N., Storvik, G., and Nedreaas, K. 2017. Latent Gaussian models to predict historical
575 bycatch in commercial fishery. *Fisheries Research* **185**: 62–72.

576 Cameletti, M., Lindgren, F., Simpson, D., and Rue, H. 2013. Spatio-temporal modeling of
577 particulate matter concentration through the SPDE approach. *AStA Adv Stat Anal*
578 **97**(2): 109–131. doi:10.1007/s10182-012-0196-3.

579 Campbell, M.S., Stehfest, K.M., Votier, S.C., and Hall-Spencer, J.M. 2014. Mapping fisheries for
580 marine spatial planning: Gear-specific vessel monitoring system (VMS), marine
581 conservation and offshore renewable energy. *Marine Policy* **45**: 293–300.
582 doi:10.1016/j.marpol.2013.09.015.

583 Cao, J., Thorson, J.T., Punt, A.E., and Szuwalski, C. 2020. A novel spatiotemporal stock
584 assessment framework to better address fine-scale species distributions:
585 development and simulation testing. *Fish and Fisheries* **21**(2): 350–367.

586 Conn, P.B., Thorson, J.T., and Johnson, D.S. 2017. Confronting preferential sampling when
587 analysing population distributions: diagnosis and model-based triage. *Methods in*
588 *Ecology and Evolution* **8**(11): 1535–1546.

589 Cornou, A.-S., Quinio-Scavinner, M., Sagan, J., Cloâtre, T., Dubroca, L., and Billet, N. 2021.
590 Captures et rejets des métiers de pêche français - Résultats des observations à bord
591 des navires de pêche professionnelle en 2019. Ifremer.

592 Cressie, N., and Wikle, C.K. 2015. *Statistics for spatio-temporal data*. John Wiley & Sons.

593 Delage, N., and Le Pape, O. 2016. Inventaire des zones fonctionnelles pour les ressources
594 halieutiques dans les eaux sous souveraineté française. Première partie: Définitions,
595 critères d'importance et méthode pour déterminer des zones d'importance à

596 protéger en priorité. Rapport de recherche, Pôle halieutique AGROCAMPUS OUEST,
597 Rennes.

598 Diggle, P.J., Menezes, R., and Su, T. 2010. Geostatistical inference under preferential
599 sampling. *Journal of the Royal Statistical Society: Series C (Applied Statistics)* **59**(2):
600 191–232.

601 Fox, C.J., Taylor, M., Dickey-Collas, M., Fossum, P., Kraus, G., Rohlf, N., Munk, P., van Damme,
602 C.J., Bolle, L.J., and Maxwell, D.L. 2008. Mapping the spawning grounds of North Sea
603 cod (*Gadus morhua*) by direct and indirect means. *Proceedings of the Royal Society*
604 *B: Biological Sciences* **275**(1642): 1543–1548.

605 Gerritsen, H., and Lordan, C. 2010. Integrating vessel monitoring systems (VMS) data with
606 daily catch data from logbooks to explore the spatial distribution of catch and effort
607 at high resolution. *ICES Journal of Marine Science* **68**(1): 245–252.

608 Getis, A., and Ord, J. 1992. The analysis of spatial association by use of distance statistics.
609 *Geographical Analysis*.

610 Girardin, R., Hamon, K.G., Pinnegar, J., Poos, J.J., Thébaud, O., Tidd, A., Vermard, Y., and
611 Marchal, P. 2017. Thirty years of fleet dynamics modelling using discrete-choice
612 models: What have we learned? *Fish and Fisheries* **18**(4): 638–655.
613 doi.org/10.1111/faf.12194.

614 Hilborn, R., and Walters, C.J. 2013. *Quantitative Fisheries Stock Assessment: Choice,*
615 *Dynamics and Uncertainty.* Springer Science & Business Media.

616 Hintzen, N.T., Aarts, G., Poos, J.J., Van der Reijden, K.J., and Rijnsdorp, A.D. 2021. Quantifying
617 habitat preference of bottom trawling gear. *ICES Journal of Marine Science* **78**(1):
618 172–184.

619 Hintzen, N.T., Bastardie, F., Beare, D., Piet, G.J., Ulrich, C., Deporte, N., Egekvist, J., and Degel,
620 H. 2012. VMStools: Open-source software for the processing, analysis and
621 visualisation of fisheries logbook and VMS data. *Fisheries Research* **115**: 31–43.
622 Elsevier.

623 Houise, C., and Forest, A. 1993. Etude de la population du Merlan (*Merlangius merlangius*
624 L.) du Golfe de Gascogne. Ifremer.

625 Hovgêrd, H., and Lassen, H. 2008. Manual on estimation of selectivity for gillnet and longline
626 gears in abundance surveys. Food & Agriculture Org.

627 ICES. 2005. Report of the Workshop on Survey Design and Data Analysis (WKSAD). Sète,
628 France.

629 ICES. 2019a. Sole (*Solea solea*) in divisions 8.a–b (northern and central Bay of Biscay).
630 Advice. Available from <https://doi.org/10.17895/ices.advice.4775>.

631 ICES. 2019b. Whiting (*Merlangius merlangus*) in Subarea 8 and Division 9.a (Bay of Biscay
632 and Atlantic Iberian waters). doi:10.17895/ICES.ADVISE.4777.

633 ICES. 2020a. Working Group on Cephalopod Fisheries and Life History (WGCEPH). ICES.
634 doi:10.17895/ICES.PUB.6032.

635 ICES. 2020b. International Bottom Trawl Survey Working Group (IBTSWG). ICES Scientific
636 Reports, ICES. Available from <http://www.ices.dk/sites/pub/Publication>
637 [Reports/Forms/DispForm.aspx?ID=37066](http://www.ices.dk/sites/pub/Publication) [accessed 28 May 2021].

638 Janßen, H., Bastardie, F., Eero, M., Hamon, K.G., Hinrichsen, H.-H., Marchal, P., Nielsen, J.R., Le
639 Pape, O., Schulze, T., and Simons, S. 2018. Integration of fisheries into marine spatial
640 planning: Quo vadis? *Estuarine, Coastal and Shelf Science* **201**: 105–113.

641 Kai, M., Thorson, J.T., Piner, K.R., and Maunder, M.N. 2017. Spatiotemporal variation in size-
642 structured populations using fishery data: an application to shortfin mako (*Isurus*

643 oxyrinchus) in the Pacific Ocean. *Canadian Journal of Fisheries and Aquatic Sciences*
644 **74**(11): 1765–1780.

645 Kristensen, K., Nielsen, A., Berg, C.W., Skaug, H., and Bell, B.M. 2016. TMB: Automatic
646 Differentiation and Laplace Approximation. *Journal of Statistical Software* **70**(1): 1–
647 21. doi:10.18637/jss.v070.i05.

648 Lambert, C., Virgili, A., Pettex, E., Delavenne, J., Toison, V., Blanck, A., and Ridoux, V. 2017.
649 Habitat modelling predictions highlight seasonal relevance of Marine Protected
650 Areas for marine megafauna. *Deep Sea Research Part II: Topical Studies in*
651 *Oceanography* **141**: 262–274.

652 Leach, C.B., Williams, P.J., Eisaguirre, J.M., Womble, J.N., Bower, M.R., and Hooten, M.B. 2021.
653 Recursive Bayesian computation facilitates adaptive optimal design in ecological
654 studies. *Ecology*: e03573.

655 Lindgren, F., Rue, H., and Lindström, J. 2011. An explicit link between Gaussian fields and
656 Gaussian Markov random fields: the stochastic partial differential equation
657 approach. *Journal of the Royal Statistical Society: Series B (Statistical Methodology)*
658 **73**(4): 423–498. Wiley Online Library.

659 Loiselle, B.A., Howell, C.A., Graham, C.H., Goerck, J.M., Brooks, T., Smith, K.G., and Williams,
660 P.H. 2003. Avoiding pitfalls of using species distribution models in conservation
661 planning. *Conservation biology* **17**(6): 1591–1600.

662 Milisenda, G., Garofalo, G., Fiorentino, F., Colloca, F., Maynou, F., Ligas, A., Musumeci, C.,
663 Bentes, L., Gonçalves, J.M.S., Erzini, K., Russo, T., D’Andrea, L., and Vitale, S. 2021.
664 Identifying Persistent Hot Spot Areas of Undersized Fish and Crustaceans in
665 Southern European Waters: Implication for Fishery Management Under the Discard
666 Ban Regulation. *Frontiers in Marine Science* **8**: 60. doi:10.3389/fmars.2021.610241.

667 Moreno, A., Pereira, J., Arvanitidis, C., Robin, J.-P., Koutsoubas, D., Perales-Raya, C., Cunha,
668 M.M., Balguerías, E., and Denis, V. 2002. Biological variation of *Loligo vulgaris*
669 (Cephalopoda: Loliginidae) in the eastern Atlantic and Mediterranean. *Bulletin of*
670 *Marine Science* **71**(1): 515–534.

671 Murray, L.G., Hinz, H., Hold, N., and Kaiser, M.J. 2013. The effectiveness of using CPUE data
672 derived from Vessel Monitoring Systems and fisheries logbooks to estimate scallop
673 biomass. *ICES Journal of Marine Science* **70**(7): 1330–1340.

674 Nielsen, J.R. 2015. Methods for integrated use of fisheries research survey information in
675 understanding marine fish population ecology and better management advice:
676 improving methods for evaluation of research survey information under
677 consideration of survey fish detection and catch efficiency. Wageningen University.

678 Nielsen, J.R., Thunberg, E., Holland, D.S., Schmidt, J.O., Fulton, E.A., Bastardie, F., Punt, A.E.,
679 Allen, I., Bartelings, H., and Bertignac, M. 2018. Integrated ecological–economic
680 fisheries models—Evaluation, review and challenges for implementation. *Fish and*
681 *Fisheries* **19**(1): 1–29.

682 Ord, J.K., and Getis, A. 1995. Local Spatial Autocorrelation Statistics: Distributional Issues
683 and an Application. *Geographical Analysis* **27**(4): 286–306. doi:10.1111/j.1538-
684 4632.1995.tb00912.x.

685 Pedersen, S.A., Fock, H.O., and Sell, A.F. 2009. Mapping fisheries in the German exclusive
686 economic zone with special reference to offshore Natura 2000 sites. *Marine Policy*
687 **33**(4): 571–590. doi:10.1016/j.marpol.2008.12.007.

- 688 Pennino, M.G., Conesa, D., Lopez-Quilez, A., Munoz, F., Fernández, A., and Bellido, J.M. 2016.
689 Fishery-dependent and-independent data lead to consistent estimations of essential
690 habitats. *ICES Journal of Marine Science* **73**(9): 2302–2310. Oxford University Press.
- 691 Pennino, M.G., Paradinas, I., Illian, J.B., Muñoz, F., Bellido, J.M., López-Quílez, A., and Conesa,
692 D. 2019. Accounting for preferential sampling in species distribution models.
693 *Ecology and evolution* **9**(1): 653–663.
- 694 Petitgas, P. 1997. Sole egg distributions in space and time characterised by a geostatistical
695 model and its estimation variance. *ICES Journal of Marine Science* **54**(2): 213–225.
- 696 Pinto, C., Travers-Trolet, M., Macdonald, J.I., Rivot, E., and Vermard, Y. 2019. Combining
697 multiple data sets to unravel the spatiotemporal dynamics of a data-limited fish
698 stock. *Canadian Journal of Fisheries and Aquatic Sciences* **76**(8): 1338–1349. NRC
699 Research Press.
- 700 Regimbart, A., Guitton, J., and Le Pape, O. 2018. Zones fonctionnelles pour les ressources
701 halieutiques dans les eaux sous souveraineté française. Deuxième partie : Inventaire.
702 Rapport d'étude. Les publications du Pôle halieutique A. Pôle halieutique
703 AGROCAMPUS OUEST, Rennes.
- 704 Rufener, M.-C., Kristensen, K., Nielsen, J.R., and Bastardie, F. 2021. Bridging the gap between
705 commercial fisheries and survey data to model the spatiotemporal dynamics of
706 marine species. *Ecological Applications*: e02453.
- 707 Salas, S., and Gaertner, D. 2004. The behavioural dynamics of fishers: management
708 implications. *Fish and Fisheries* **5**(2): 153–167. doi:[https://doi.org/10.1111/j.1467-
709 2979.2004.00146.x](https://doi.org/10.1111/j.1467-2979.2004.00146.x).
- 710 Silvano, R.A., MacCord, P.F., Lima, R.V., and Begossi, A. 2006. When does this fish spawn?
711 Fishermen's local knowledge of migration and reproduction of Brazilian coastal
712 fishes. *Environmental Biology of fishes* **76**(2): 371–386.
- 713 Stock, B.C., Ward, E.J., Thorson, J.T., Jannot, J.E., and Semmens, B.X. 2019. The utility of
714 spatial model-based estimators of unobserved bycatch. *ICES Journal of Marine
715 Science* **76**(1): 255–267. doi:10.1093/icesjms/fsy153.
- 716 Thorson, J.T. 2018. Three problems with the conventional delta-model for biomass
717 sampling data, and a computationally efficient alternative. *Canadian Journal of
718 Fisheries and Aquatic Sciences* **75**(9): 1369–1382. NRC Research Press.
- 719 Thorson, J.T., Adams, C.F., Brooks, E.N., Eisner, L.B., Kimmel, D.G., Legault, C.M., Rogers, L.A.,
720 and Yasumiishi, E.M. 2020a. Seasonal and interannual variation in spatio-temporal
721 models for index standardization and phenology studies. *ICES Journal of Marine
722 Science* **77**(5): 1879–1892.
- 723 Thorson, J.T., Ciannelli, L., and Litzow, M.A. 2020b. Defining indices of ecosystem variability
724 using biological samples of fish communities: A generalization of empirical
725 orthogonal functions. *Progress in Oceanography* **181**: 102244.
726 doi:10.1016/j.pocean.2019.102244.
- 727 Tidd, A.N., Vermard, Y., Marchal, P., Pinnegar, J., Blanchard, J.L., and Milner-Gulland, E.J.
728 2015. Fishing for Space: Fine-Scale Multi-Sector Maritime Activities Influence Fisher
729 Location Choice. *PLOS ONE* **10**(1): e0116335. doi:10.1371/journal.pone.0116335.
- 730 Vermard, Y., Marchal, P., Mahévas, S., and Thébaud, O. 2008. A dynamic model of the Bay of
731 Biscay pelagic fleet simulating fishing trip choice: the response to the closure of the
732 European anchovy (*Engraulis encrasicolus*) fishery in 2005. *Can. J. Fish. Aquat. Sci.*
733 **65**(11): 2444–2453. doi:10.1139/F08-147.

- 734 Wikle, C.K., Zammit-Mangion, A., and Cressie, N. 2019. Spatio-temporal Statistics with R.
735 CRC Press.
- 736 Yan, Y., Cantoni, E., Field, C., Treble, M., and Flemming, J.M. 2022. Spatiotemporal modeling
737 of bycatch data: methods and a practical guide through a case study in a Canadian
738 Arctic fishery. *Canadian Journal of Fisheries and Aquatic Sciences* **79**(1): 148–158.
- 739 Yochum, N., Starr, R.M., and Wendt, D.E. 2011. Utilizing fishermen knowledge and expertise:
740 keys to success for collaborative fisheries research. *Fisheries* **36**(12): 593–605.
741

742 **TABLES**

743

744

745

Table 1. Ratio between the negative log-likelihood values (either commercial or scientific) from the IM accounting for PS and the IM ignoring PS.

Species	Negative log-likelihood ratio	
	Scientific data	Commercial data
Sole	0.97	0.92
Squids	1.00	1.01
Whiting	0.99	1.00

746

747

748

Note. The ratio between negative log-likelihoods ($-\log(\mathit{ll})$) is given as: $r = \frac{-\log(\mathit{ll}_{PS})}{-\log(\mathit{ll}_{noPS})}$.
 If $r < 1$, the model accounting for PS better fits the data than the model ignoring PS (no PS).

749

FIGURES CAPTION

750 Figure 1. Spatial distribution of each fleet on the whole period (2010-2018). Unit: fishing
751 effort in fishing hour.

752

753 Figure 2. Diagram of the integrated spatio-temporal model.

754

755 Figure 3. Comparison between the observed scientific CPUE (y-axis) and the
756 corresponding model predictions (x-axis) on the month of the survey, based on model
757 integrating data from one commercial fleet only (either OTB_CEP, OTB_DEF, OTT_DEF)
758 or from all commercial fleets (Integrated model). x-axis: model predictions. y-axis:
759 scientific data observations (CPUE in kg/hour). Black line: linear regression 'log(scientific
760 observations) ~ log(model predictions)'. r : Spearman correlation coefficient. Scientific data
761 are integrated to inference for all models.

762

763 Figure 4. Sole case study. Comparison between predictions from the integrated model
764 (using all fishing fleets) and the model integrating only one commercial fleet for the 12
765 months of year 2018. Left: OTB_CEP fleet, middle: OTB_DEF fleet, right: OTT_DEF fleet.
766 x-axis: integrated model predictions. y-axis: single-fleet model predictions. The prediction
767 values are log-scaled. Red points: predictions within the sampling area of the related fleets
768 (i.e. the cells sampled by the fleet). Black points: predictions outside the sampling area of
769 the related fleets. Black line: $x = y$ axis. Note that the intercept of the x-y line has been
770 scaled to account for differences in the intercept values between models. Scientific data
771 are integrated to inference for all models.

772

773 Figure 5. Estimates of PS parameters for each commercial fleet (left) and effect of PS
774 on model outputs (right). Left: boxplot represent the variability of maximum likelihood
775 estimates of parameters b across the monthly time steps. Right: log-predictions of the
776 integrated model accounting for PS (y-axis) versus log-predictions of the integrated model
777 ignoring PS (x-axis) for the 12 months of year 2018. Blue points: predictions within the
778 sampling area of the commercial fleets (i.e. the cells sampled by commercial fleets). Black
779 point: predictions outside the sampling area of the commercial fleets. Black line: $x = y$
780 axis.

781

782 Figure 6. Sole case study. (Top) Temporal evolution of the b parameters for the three
783 commercial fleets fitted to the integrated model. Blue vertical lines: January. (Bottom)
784 Monthly biomass distribution averaged on the full period. Only quantile values are
785 represented. Model predictions come from the integrated model accounting for PS.

786

787 Figure 7. Left: index of persistence during the reproduction period of sole (February),
788 whiting (March-May) and squids (January-April). Reproduction period defined from

789 ecological expertise. Index were computed from 2010 to 2018. Right: literature information
790 on reproduction grounds when available. For sole, the map represents egg concentration
791 from an egg and larvae survey conducted in 1982 (Arbault et al., 1986). For whiting, the
792 map represents records of age-2+ whiting (i.e. mature individuals), from two spring trawl
793 surveys that occurred between 1987 and 1992 (House and Forest, 1993). Model
794 predictions come from the integrated model accounting for PS.

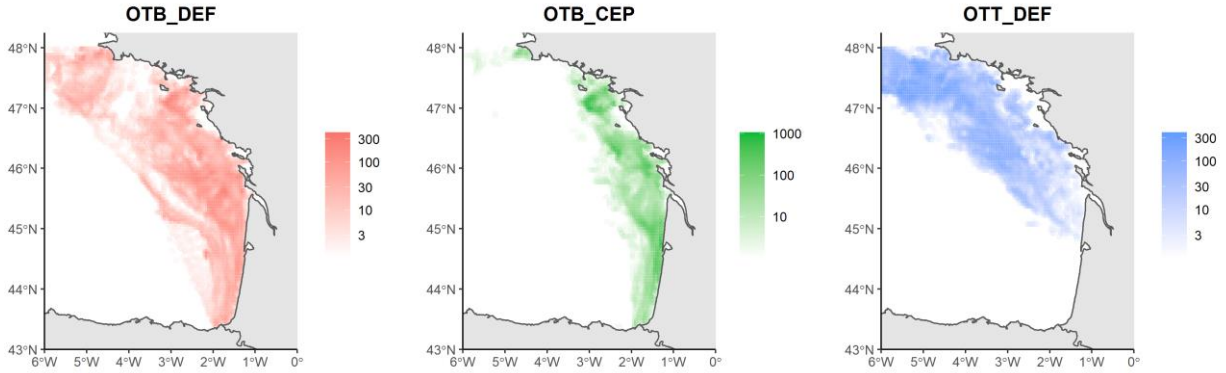
795
796 Figure 8. Persistence indices within the reproduction period computed on a 5-year mobile
797 time-span for each 3 species (5-year time span indicated on the top of each map). Model
798 predictions come from the integrated model accounting for PS.

799

800

801 FIGURES

802



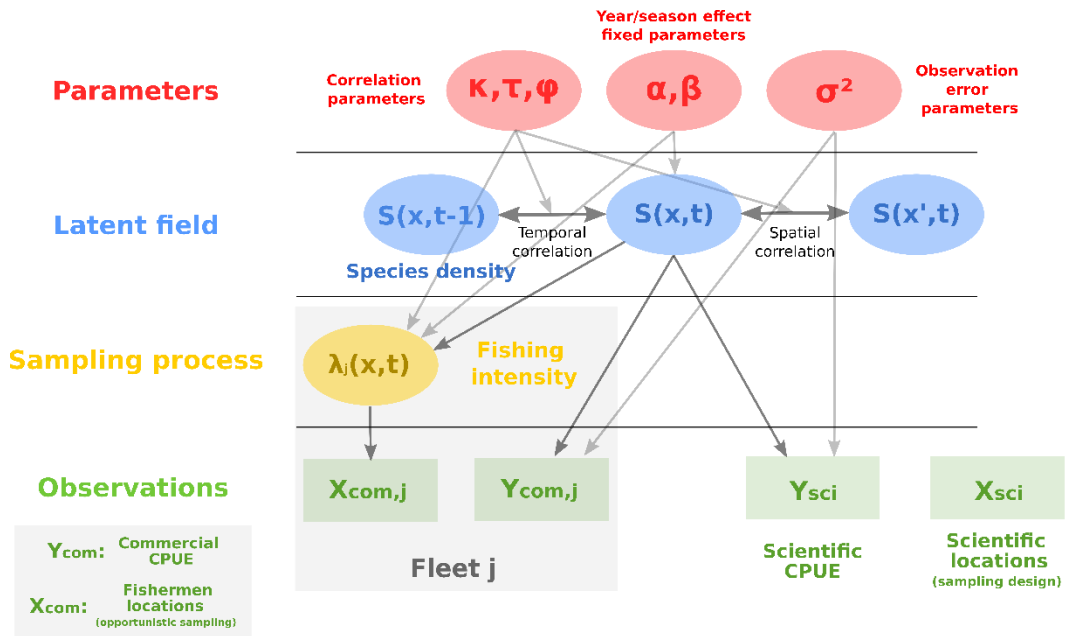
803

804

805

806

Figure 1



807

808

809

Figure 2

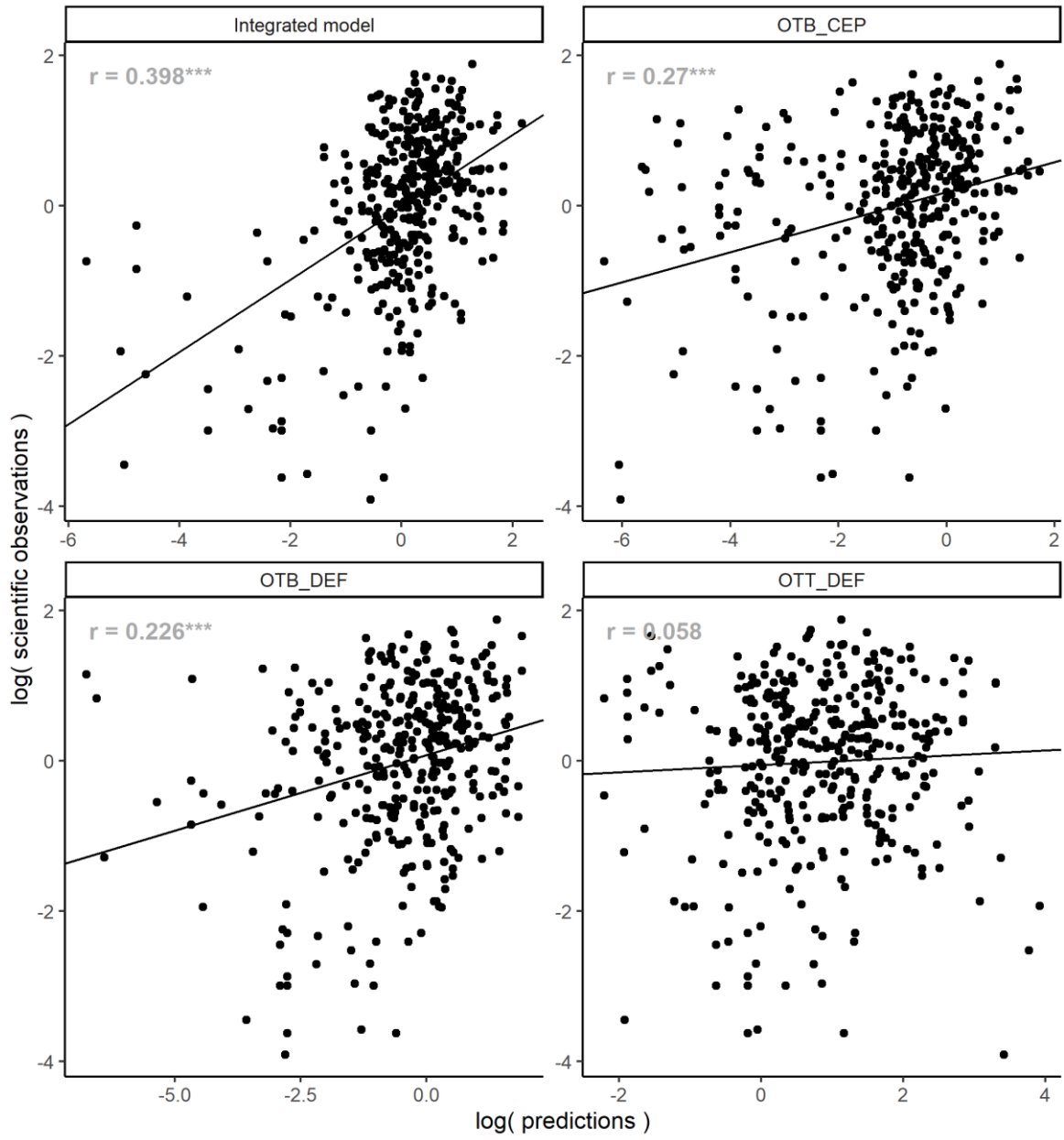


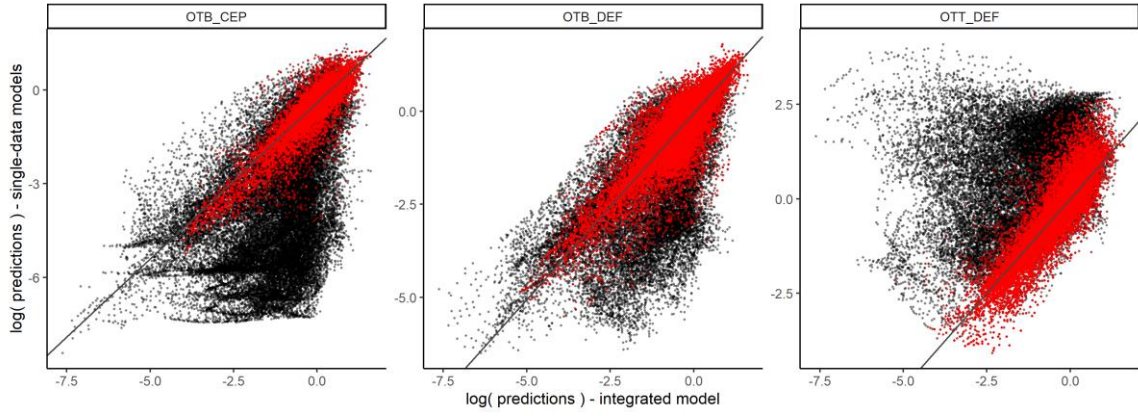
Figure 3

810

811

812

813



814

815

Figure 4

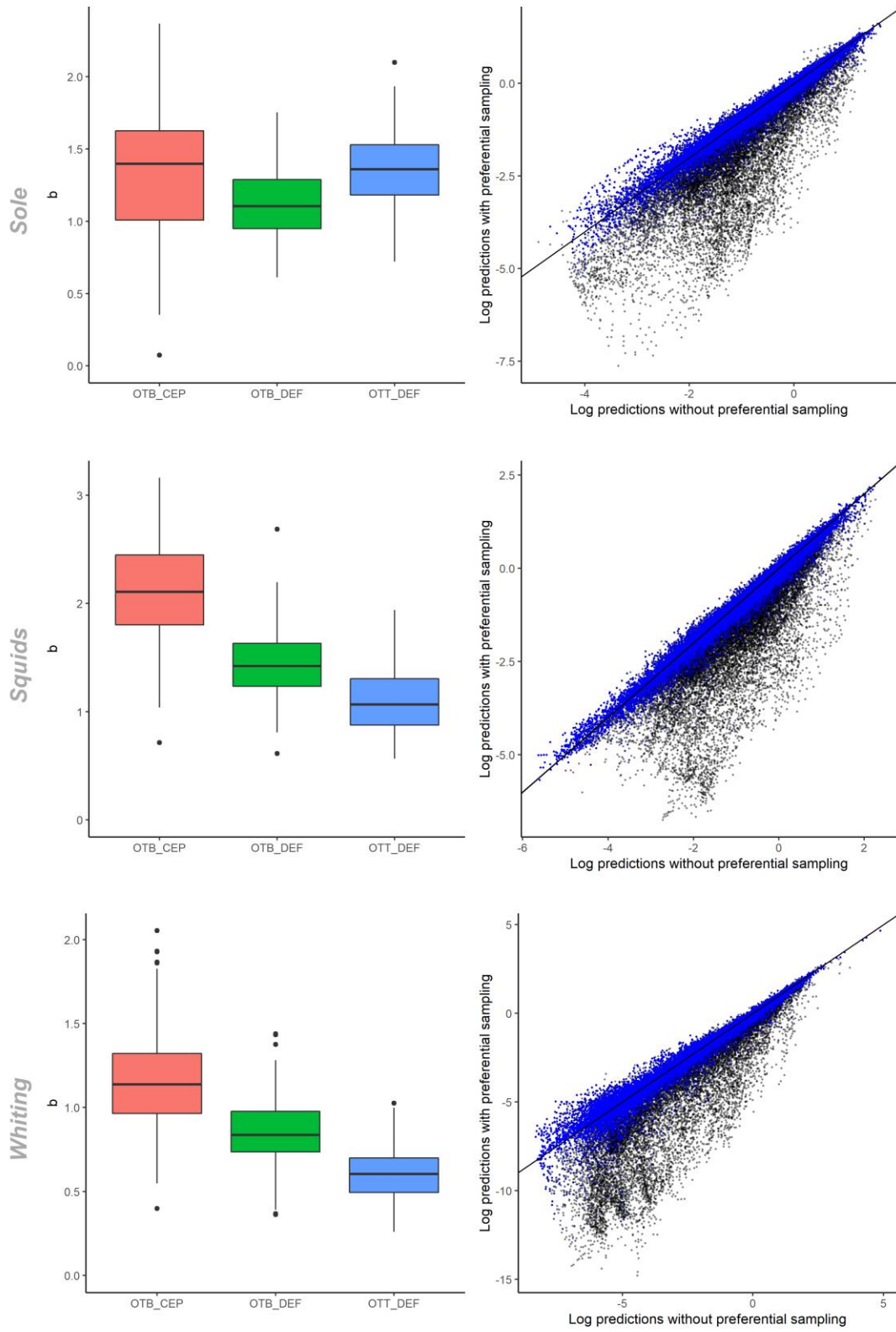
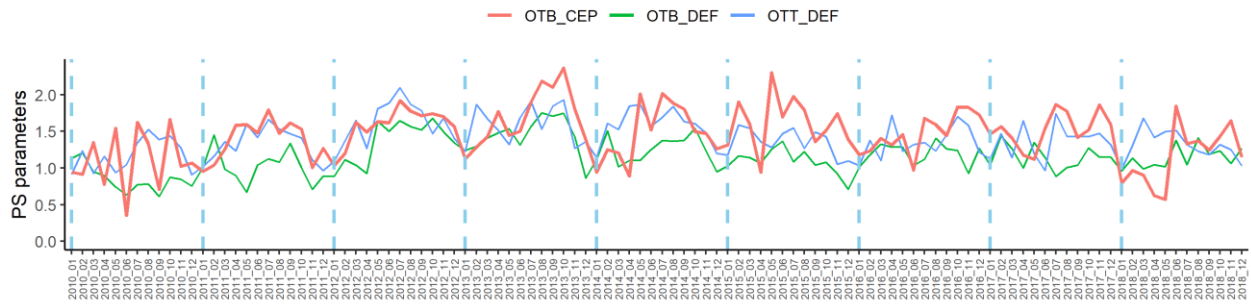


Figure 5

816
817
818

Sole case study



Monthly mean distribution

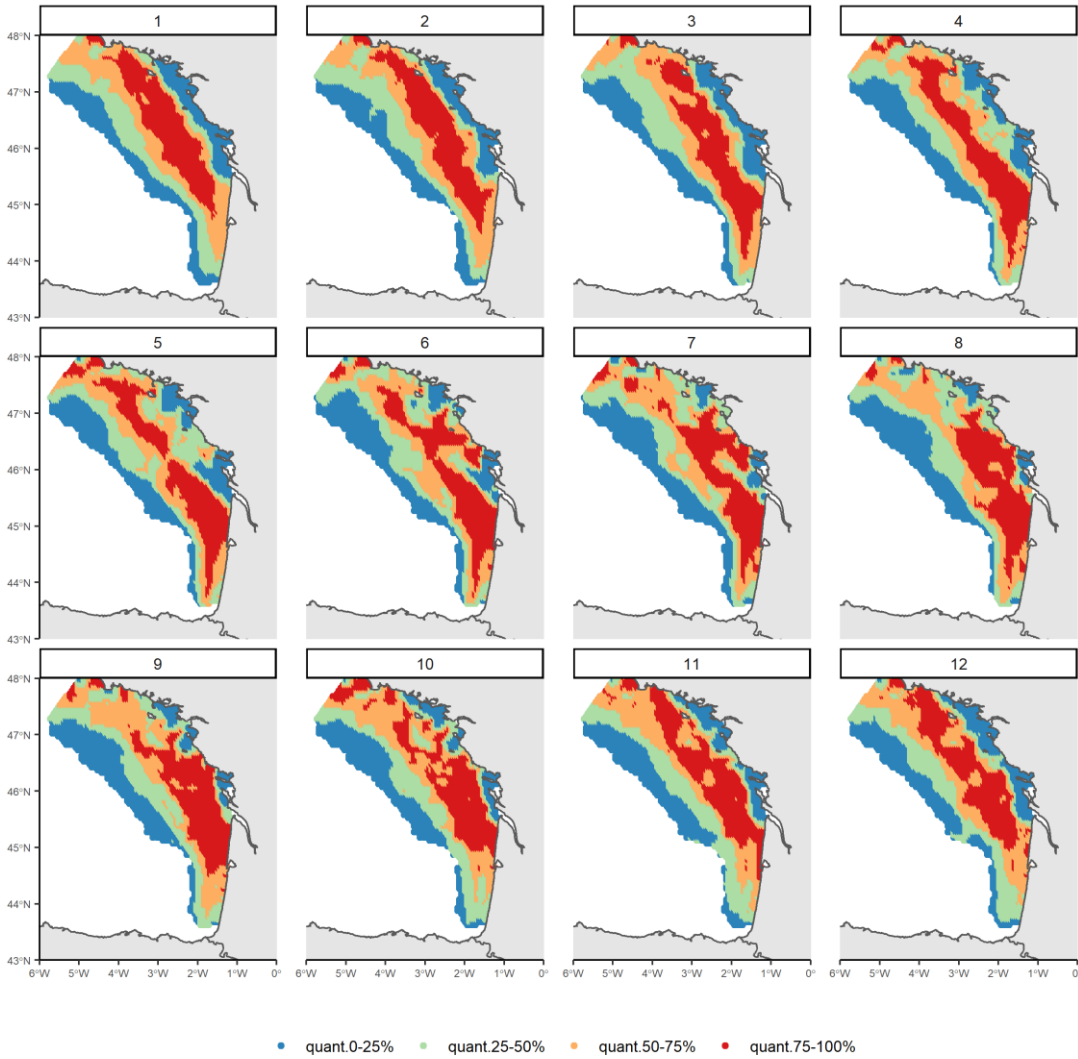
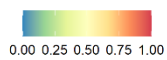
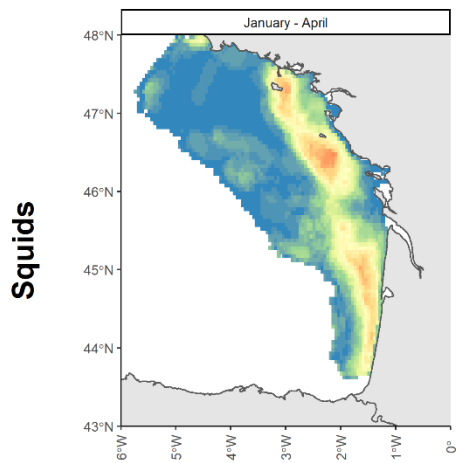
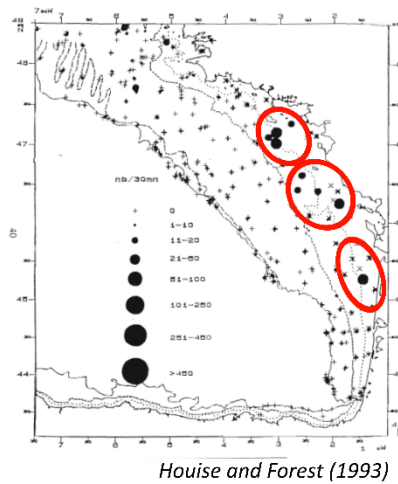
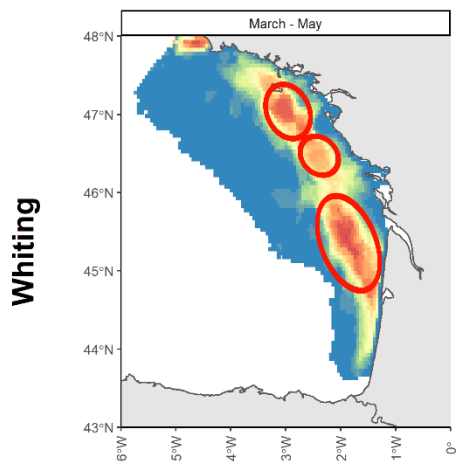
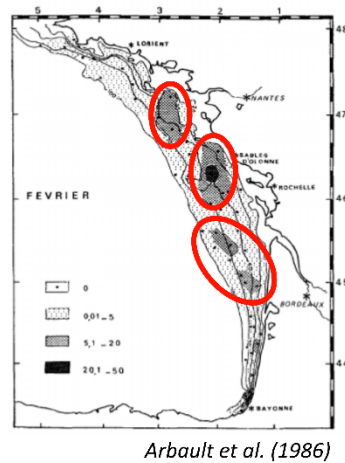
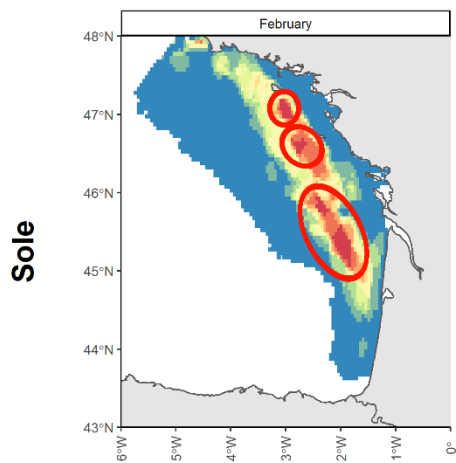


Figure 6

819
820
821

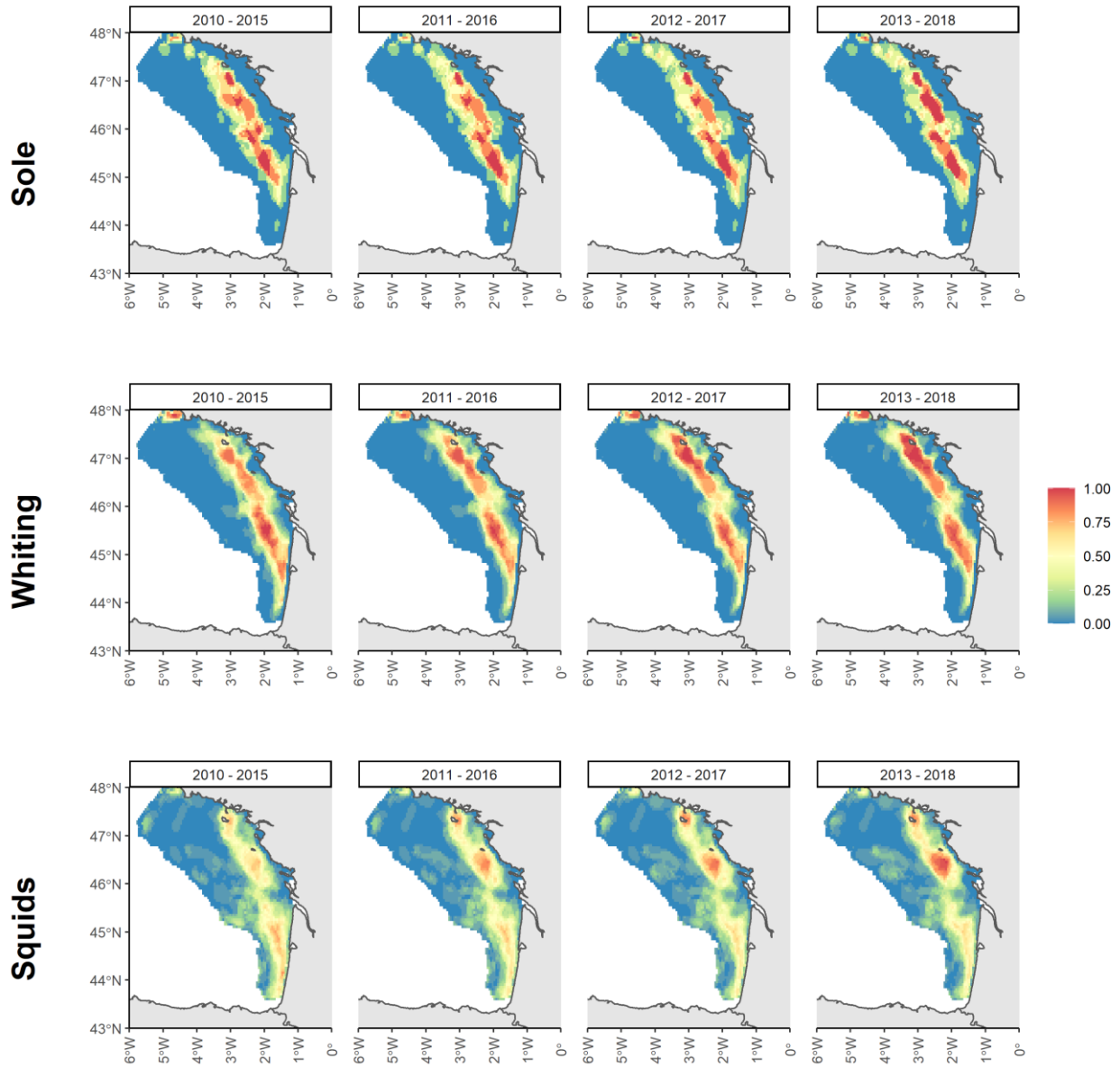


822

823

Figure 7

824



825

826

Figure 8

827 **APPENDICES**

828 The appendices are in the supplementary material file.